

## Conductivity hysteresis in polymer electrolytes incorporating poly(tetrahydrofuran)

Ozge Akbulut<sup>a</sup>, Ikuo Taniguchi<sup>a</sup>, Sundeep Kumar<sup>b</sup>, Yang Shao-Horn<sup>b</sup>, Anne M. Mayes<sup>a,\*</sup>

<sup>a</sup> Department of Materials Science and Engineering, Massachusetts Institute of Technology, Cambridge, MA 02139-4307 USA

<sup>b</sup> Department of Mechanical Engineering, Massachusetts Institute of Technology, Cambridge, MA 02139-4307 USA

Received 12 May 2006; received in revised form 1 August 2006; accepted 9 August 2006

Available online 9 October 2006

### Abstract

Conductivity hysteresis and room temperature ionic conductivities  $>10^{-3}$  S/cm were recently reported for electrolytes prepared from blends of an amphiphilic comb copolymer, poly[2,5,8,11,14-pentaoxapentadecamethylene (5-hexadecyloxy-1,3-phenylene)] (polymer I), and a linear multiblock copolymer, poly(oligotetrahydrofuran-*co*-dodecamethylene) (polymer II), following thermal treatment [F. Chia, Y. Zheng, J. Liu, N. Reeves, G. Ungar, P.V. Wright, *Electrochim. Acta* 43 (2003) 1939]. To investigate the origin of these effects, polymers I and II were synthesized in this work, and the conductivity and thermal properties of the individual polymers were investigated. AC impedance measurements were conducted on I and II doped with LiBF<sub>4</sub> or LiClO<sub>4</sub> during gradual heating to 110 °C and slow cooling to room temperature. Significant conductivity hysteresis was seen for polymer II, and was similarly observed for poly(tetrahydrofuran) (PTHF) homopolymer at equivalent doping levels. From thermogravimetric analysis (TGA), gel permeation chromatography (GPC) and <sup>1</sup>H NMR spectroscopy, both polymer II and PTHF were found to partially decompose to THF during heat treatment, resulting in a self-plasticizing effect on conductivity.

© 2006 Elsevier Ltd. All rights reserved.

**Keywords:** Polymer electrolytes; Conductivity hysteresis; Poly(tetrahydrofuran); Lithium battery; Self-assembly

### 1. Background

Solvent free polymer electrolytes have gained wide attention as potential replacements for liquid electrolytes that currently limit the thermal stability, energy density and safety of commercial secondary lithium cells [1]. Extensive research has been conducted on variants of poly(ethylene oxide), PEO, the first polymer discovered to exhibit substantial ionic conductivity when doped with alkali salts [2], in an effort to boost room temperature ionic conductivity of dry polymer electrolytes to values sufficient for battery applications[3–6]. Despite substantial efforts, ambient conductivities for dry polymer electrolytes appear to have reached a plateau at  $10^{-4}$  to  $10^{-5}$  S/cm for PEO derivatives doped with lithium bis(trifluoromethanesulfone)imide, LiTFSI [1].

As one surprising exception, Wright and co-workers [7–9] recently reported the preparation of polymer blend electrolytes exhibiting room temperature conductivities  $>10^{-3}$  S/cm after

thermal treatment. The Wright blends are comprised of an amphiphilic comb copolymer, poly[2,5,8,11,14-pentaoxapentadecamethylene(5-hexadecyloxy-1,3-phenylene)] (polymer I), and a linear multiblock copolymer, poly(oligotetrahydrofuran-*co*-dodecamethylene) (polymer II), whose structures are given in Fig. 1. Although these materials, when blended at roughly 50/50 (w/w) and doped with lithium salts ( $\sim 12:1$  ether oxygen:Li) gave initial room temperature conductivities of  $10^{-7}$  to  $10^{-8}$  S/cm, their conductivities rose with heating to  $>10^{-3}$  S/cm at  $\sim 110$  °C. The high temperature conductivity values were substantially retained upon subsequently cooling to room temperature.

The uniquely high ambient conductivities reported for these systems after heat treatment have been suggested to result from the decoupling of Li<sup>+</sup> ion motion from that of polymer I as a consequence of its self-assembly into liquid crystalline domains of alkyl side chains housing helical ion conducting channels formed from the polyether backbone. Deblending of I and II by heating above the liquid crystal-isotropic transition temperature ( $T_{\text{iso}} \sim 110$  °C) was suggested to facilitate ion conduction, with polymer II regions serving as ion bridges between liquid crystalline domains of polymer I upon cooling [7–9].

\* Corresponding author. Tel.: +1 617 253 3318; fax: +1 617 452 3432.  
E-mail address: [amayes@mit.edu](mailto:amayes@mit.edu) (A.M. Mayes).

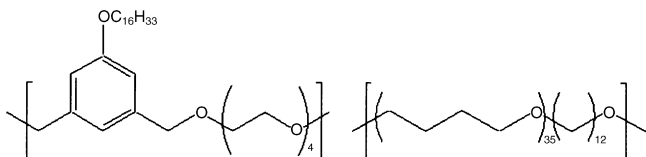


Fig. 1. Chemical structures of: (a) poly[2,5,8,11,14-pentaoxapentadecamethylene (5-hexadecyloxy-1,3-phenylene)] (polymer I) and (b) poly(oligotetrahydrofuran-co-dodecamethylene) (polymer II).

To further explore the origin of the weekly temperature dependent conductivity after thermal cycling reported for the systems developed by Wright and co-workers, polymers I and II were synthesized in this work and the conductivity and thermal properties of the individual copolymers investigated. The conductivity hysteresis in these systems could be attributed to polymer II, which incorporates polytetrahydrofuran (PTHF) as its ion-conducting component. PTHF homopolymer was then synthesized and found to display similar conductivity hysteresis. Both polymer II and PTHF were found by differential scanning calorimetry (DSC) to exhibit a high melting point phase ( $T_{\text{endo}} \sim 95\text{--}110\text{ }^{\circ}\text{C}$ ) when doped with  $\text{LiClO}_4$  or  $\text{LiBF}_4$ , which does not re-crystallize readily on cooling, indicating that an amorphous phase with high salt content is present at ambient temperatures after heat treatment. However, thermogravimetric analysis (TGA), gel permeation chromatography and  $^1\text{H}$  NMR spectroscopy of both polymer II and PTHF demonstrate the formation of significant fractions of THF by decomposition during heat treatment. The THF component generated on heating appears to serve as a plasticizer in these systems, conveying liquid-like conductivity to the electrolyte.

## 2. Experimental

### 2.1. Materials

5-Hydroxyisophthalic acid, 1-bromohexadecane, triphenylphosphine, tetraethylene glycol, poly(tetramethylene oxide), 1,12-dibromododecane, and 1 M  $\text{LiAlH}_4$  in THF solution were purchased from Aldrich (MO, USA). THF for PTHF synthesis was refluxed with lithium aluminum hydride for several hours, and then distilled over sodium. Other anhydrous solvents were obtained from Aldrich and used as received. Other organic and inorganic materials were reagent grade and used without further purification.

Synthesis of polymers I and II were carried out based on previous reports [7–16].

#### 2.1.1. Synthesis of diethyl 5-hydroxyisophthalate

A 37 g (203 mmol) quantity of 5-hydroxyisophthalic acid and 2 mL of concentrated sulfuric acid were added to 150 mL ethanol, and the mixture was refluxed for several hours. Ethanol was removed by evaporation, and the resulting white precipitate was washed with deionized water. The precipitate was dissolved in ethyl acetate and further washed with aqueous sodium hydrogen carbonate. The organic phase was dried with magnesium sulfate. Finally, the product was obtained by evaporation with

93% yield.  $^1\text{H}$  NMR (400 MHz in  $\text{CDCl}_3$ ),  $\delta$  (ppm): 1.41 (t, 6H,  $\text{CH}_3$ ), 4.41 (q, 4H,  $\text{CH}_2$ ), 7.82 (s, 2H, CH), and 8.23 (s, 1H, CH).

#### 2.1.2. Synthesis of diethyl 5-hexadecyloxyisophthalate

A 43.0 g (181 mmol) quantity of diethyl 5-hydroxyisophthalate, 72.1 g (236 mmol) of 1-bromohexadecane, and 32.6 g (236 mmol) potassium carbonate were refluxed in 300 mL acetone for 72 h. The mixture was filtered and condensed by evaporation. Water and pentane were added to the condensate to extract the product into the organic phase. The organic phase was dried with magnesium sulfate and the product obtained by evaporation with 68% yield.  $^1\text{H}$  NMR (400 MHz in  $\text{CDCl}_3$ ),  $\delta$  (ppm): 0.87 (t, 3H,  $\text{OC}_{15}\text{H}_{30}\text{CH}_3$ ), 1.25–1.30 (m, 26H,  $\text{OC}_2\text{H}_4\text{C}_{13}\text{H}_{26}\text{CH}_3$ ), 1.40 (t, 6H,  $\text{OCH}_2\text{CH}_3$ ), 1.80 (m, 2H,  $\text{OCH}_2\text{CH}_2\text{C}_{14}\text{H}_{29}$ ), 4.03 (t, 2H,  $\text{OCH}_2\text{C}_{15}\text{H}_{31}$ ), 4.40 (q, 4H,  $\text{OCH}_2\text{CH}_3$ ), 7.74 (s, 2H, CH), and 8.25 (s, 1H, CH).

#### 2.1.3. Synthesis of 5-hexadecyloxybenzene-1,3-dimethanol

A 30.0 g (64.9 mmol) measure of 5-hexadecyloxyisophthalate was dissolved in 500 mL anhydrous ethyl ether. To this solution was added 100 mL of 1 M  $\text{LiAlH}_4/\text{THF}$  solution. After overnight stirring, 230 mL of ethyl acetate was added to deactivate excess  $\text{LiAlH}_4$ , and saturated aqueous sodium sulfate was added. The organic phase was collected and dried with magnesium sulfate. The organic solvent was removed by evaporation and the resulting product was recrystallized in dichloromethane with 79% yield.  $^1\text{H}$  NMR (400 MHz in  $\text{CDCl}_3$ ),  $\delta$  (ppm): 0.88 (t, 3H,  $\text{OC}_{15}\text{H}_{30}\text{CH}_3$ ), 1.25–1.30 (m, 26H,  $\text{OC}_2\text{H}_4\text{C}_{13}\text{H}_{26}\text{CH}_3$ ), 1.77 (m, 2H,  $\text{OCH}_2\text{CH}_2\text{C}_{14}\text{H}_{29}$ ), 3.97 (t, 2H,  $\text{OCH}_2\text{C}_{15}\text{H}_{31}$ ), 4.66 (d, 4H,  $\text{CH}_2\text{OH}$ ), 6.84 (s, 2H, CH), and 6.93 (s, 1H, CH).

#### 2.1.4. Synthesis of

##### 1,3-bis(bromomethyl)-5-hexadecyloxybenzene

A 10.0 g (26.5 mmol) quantity of 5-hexadecyloxybenzene-1,3-dimethanol was suspended in 40 mL anhydrous ethyl ether. To the solution was added 6.36 g (23.5 mmol) of triphenylphosphine, and the mixture was first stirred at ambient temperature for 10 h and refluxed for another 12 h. The resulting reaction mixture was diluted with dichloromethane, and washed sequentially with 10% aqueous sodium carbonate and water. The organic phase was dried with magnesium sulfate, and finally the product was obtained by evaporation with 61% yield.  $^1\text{H}$  NMR (400 MHz in  $\text{CDCl}_3$ ),  $\delta$  (ppm): 0.88 (t, 3H,  $\text{OC}_{15}\text{H}_{30}\text{CH}_3$ ), 1.3–1.5 (m, 26H,  $\text{OC}_2\text{H}_4\text{C}_{13}\text{H}_{26}\text{CH}_3$ ), 1.76 (m, 2H,  $\text{OCH}_2\text{CH}_2\text{C}_{14}\text{H}_{29}$ ), 3.95 (t, 2H,  $\text{OCH}_2\text{C}_{15}\text{H}_{31}$ ), 4.43 (s, 4H,  $\text{CH}_2\text{Br}$ ), 6.86 (s, 2H, CH), and 6.98 (s, 1H, CH).

#### 2.1.5. Synthesis of polymer I

A 5.04 g (10 mmol) quantity of 1,3-bromomethane-5-hexadecyloxybenzene and 1.94 g (10 mmol) of tetraethylene glycol were dissolved in 10 mL DMSO/THF (50:50, v/v) in a 100 mL round-bottom flask. A 4.48 g (80 mmol) measure of potassium hydroxide was added to the solution, and the resulting mixture was stirred at  $60\text{ }^{\circ}\text{C}$  under nitrogen atmosphere for a week. The resulting polymer was precipitated in methanol. The precipitate was redissolved in THF and reprecipitated in

water. Finally, the polymer was dissolved in dichloromethane and purified by passing through a Celite 545 (EMD, Darmstadt, Germany) column several times to obtain a clear solution. The organic solvent was removed by evaporation resulting in a 23% yield.  $^1\text{H}$  NMR (400 MHz in  $\text{CDCl}_3$ ),  $\delta$  (ppm): 0.87 (t, 3H,  $\text{OC}_{15}\text{H}_{30}\text{CH}_3$ ), 1.3–1.5 (m, 26H,  $\text{OC}_2\text{H}_4\text{C}_{13}\text{H}_{26}\text{CH}_3$ ), 1.75 (m, 2H,  $\text{OCH}_2\text{CH}_2\text{C}_{14}\text{H}_{29}$ ), 3.58–3.73 (m, 16H,  $\text{OCH}_2\text{CH}_2\text{O}$ ), 3.93 (t, 2H,  $\text{OCH}_2\text{C}_{15}\text{H}_{31}$ ), 4.50 (s, 4H,  $\text{CCH}_2\text{OCH}_2$ ), 6.80 (s, 2H, CH), and 6.83 (s, 1H, CH). The weight average molecular weight and polydispersity index were 44 kg/mol and 1.4, respectively, based on GPC with polystyrene (PS) calibration standards.

### 2.1.6. Synthesis of polymer II

A 10.02 g (5.00 mmol) quantity of poly(tetramethylene oxide) (MW: 2 kg/mol), 1.64 g (5.00 mmol) of 1,12-dibromododecane, and 2.24 g (40 mmol) of potassium hydroxide were stirred in a 200 mL round-bottom flask under nitrogen atmosphere at  $70^\circ\text{C}$  for 2 weeks. The polymer was purified by the same methods described above with 20% yield.  $^1\text{H}$  NMR (400 MHz in  $\text{CDCl}_3$ ),  $\delta$  (ppm): 1.22–1.35 ( $\text{CH}_2\text{C}_{10}\text{H}_{20}\text{CH}_2$ ), 1.5–1.7 ( $\text{OCH}_2\text{CH}_2\text{CH}_2\text{CH}_2$ ), and 3.35–3.48 ( $\text{OCH}_2\text{CH}_2\text{CH}_2\text{CH}_2$ ,  $\text{CH}_2\text{C}_{10}\text{H}_{20}\text{CH}_2$ ). The incorporation ratio of tetramethylene oxide and dodecane units was 35:1. The weight average molecular weight and polydispersity index were 39 kg/mol and 2.4, respectively.

### 2.1.7. Synthesis of high molecular weight PTHF

High molecular weight PTHF was prepared by cationic ring-opening polymerization of THF with trifluoromethanesulfonic anhydride under anhydrous conditions. To a previously flamed 100 mL round bottom flask containing a magnetic stir bar was charged 30 mL (26.7 g, 370 mmol) of purified THF. A 44  $\mu\text{L}$  (370  $\mu\text{mol}$ ) quantity of trifluoromethanesulfonic anhydride was added through a three-way stopcock under dry nitrogen flush. The reaction mixture was stirred at ambient temperature. After several hours stirring, the stir bar ceased to rotate and dichloromethane was added to dissolve the product. The polymer was purified by reprecipitation in methanol to obtain a yield of 95%.  $^1\text{H}$  NMR (400 MHz in  $\text{CDCl}_3$ ),  $\delta$  (ppm): 1.62 ( $\text{OCH}_2\text{CH}_2\text{CH}_2\text{CH}_2$ ) and 3.41 ( $\text{OCH}_2\text{CH}_2\text{CH}_2\text{CH}_2$ ). The weight average molecular weight and polydispersity index were 405 kg/mol and 1.1, respectively.

### 2.2. Electrolyte film preparation

All polymers synthesized were kept in an argon filled glove box with  $\text{O}_2$  level below 2 ppm and humidity level below 1 ppm. Polymer–salt complexes were prepared by dissolving the corresponding polymer in anhydrous THF and the appropriate molar portion of salt in anhydrous acetonitrile in separate vials inside the glove box. After full dissolution was observed in both vials, the two solutions were mixed together under constant mechanical stirring for 6 h. Thereafter, the mixed solution was poured into a 6 cm diameter Teflon dish. After removing the excess solvent via evaporation in the glove box for several hours, the complexes were further dried under vacuum at  $50^\circ\text{C}$  for 15–18 h to remove residual solvent. Residual THF and acetonitrile con-

tents for a PTHF electrolyte so-prepared were determined by  $^1\text{H}$  NMR to be 1.4 and 0.6 wt%, respectively. The low initial room temperature conductivities of the complexes obtained indicate that any residual solvent played a minimal role in the conductivity. Doping levels are reported as ratios of ether oxygen groups to lithium ions (EO:Li) and are comparable to those used by Wright and co-workers [7,9–14].

*Thermal analysis* of the materials was conducted on a TA Instruments, Inc., 2920 DSC using a heating/cooling rate of  $10^\circ\text{C}/\text{min}$  in tightly sealed aluminum crucibles under a helium atmosphere. Thermogravimetric analysis (TGA) was performed with a TA Instruments, Inc., Q50 under nitrogen purge with a flow rate of 90 mL/min and using a platinum sample holder.

### 2.3. Conductivity measurements

The cell used for conductivity measurements consisted of two 15 mm diameter stainless steel flat electrodes, which were held inside a Teflon jacket and contained within a stainless steel cylinder. One of the electrodes was fixed and the movement of the second electrode was controlled by a micrometer, which was used to precisely control the thickness of the sample during the measurement. The polymer electrolyte sample was loaded in the conductivity cell inside an Ar filled glove box (oxygen level less than 2 ppm and moisture level less than 5 ppm). The typical sample thickness was in the range of 0.5–1 mm. The conductivity cell was finally sealed with Kapton film and electrically insulating tape to prevent any leakage of silicone oil into the cell during thermal treatment. Cross-plane conductivities of the polymer electrolytes were measured by impedance spectroscopy using a Solartron 1260 impedance gain/phase analyzer (Solartron Instruments, Allentown, PA) over a frequency range of  $10^6$ –0.1 Hz at 10 mV amplitude. Ten points per decade of frequency were collected going from high to low frequency with a temperature interval spanning 25–110  $^\circ\text{C}$ . The temperature was controlled manually using a silicone oil bath and impedance measurements were taken after equilibrating the cell typically for 2–3 h.

## 3. Results and discussion

Fig. 2 illustrates representative data for the temperature dependence of the conductivity of polymer I complexed with  $\text{LiClO}_4$  and  $\text{LiBF}_4$  at EO:Li ratios of 5:1. Although polymer I doped with  $\text{LiClO}_4$  exhibits a room temperature conductivity more than two orders of magnitude below that of the polymer I: $\text{LiBF}_4$  complex, both systems have conductivities above  $10^{-5}$  S/cm at 110  $^\circ\text{C}$ . Minimal hysteresis in the measured conductivity for polymer I complexes was observed as temperature was lowered slowly to room temperature. The room temperature conductivity of the polymer I: $\text{LiClO}_4$  complex increased from  $5.9 \times 10^{-11}$  to  $7.4 \times 10^{-11}$  S/cm (25%), while that of the polymer I: $\text{LiBF}_4$  complex increased from  $2.0 \times 10^{-8}$  to  $7.2 \times 10^{-8}$  S/cm (260%). Conductivity values upon first heating are consistent with those reported by Wright's group of  $\sim 10^{-4}$  S/cm at 110  $^\circ\text{C}$  for polymer I: $\text{LiClO}_4$  electrolytes with

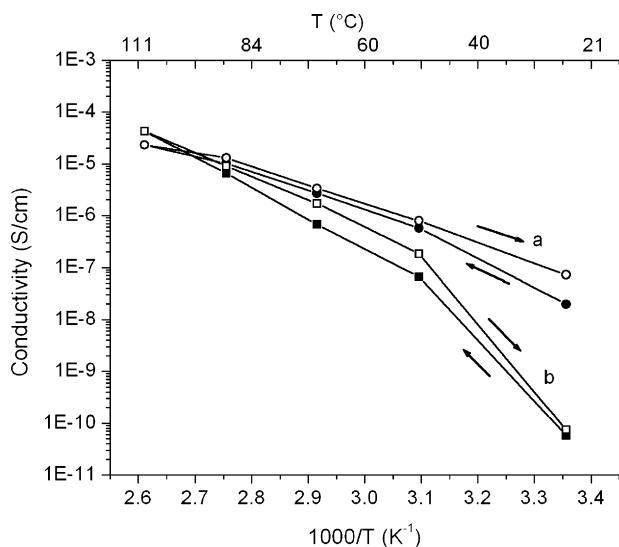


Fig. 2. Conductivity of polymer I. (a) I: LiBF<sub>4</sub> (EO:Li = 5:1); (●) heating, (○) cooling; (b) I: LiClO<sub>4</sub> (EO:Li = 5:1), (■) heating, (□) cooling.

an EO:Li ratio 5:1 [12,13]. Conductivity data upon subsequent cooling were not reported in these previous studies.

Fig. 3 displays data from a similar experiment performed on polymer II at EO:Li doping levels of 5.8:1. Little hysteresis was seen for polymer II doped with LiClO<sub>4</sub> during heating and cooling. By contrast, a dramatic rise in the room temperature conductivity from  $\sim 10^{-8}$  to  $>10^{-4}$  S/cm was found after heating and cooling the polymer II:LiBF<sub>4</sub> electrolyte. The observed hysteresis in conductivity after thermal treatment is strikingly similar to data reported by Wright and co-workers for salt-complexed blends of polymers I and II. These authors also recently reported strong hysteresis for polymer II:LiBF<sub>4</sub> doped to an EO:Li ratio of 5.8:1. [9] Taken together, the data presented in Figs. 2 and 3 led us to hypothesize that polymer II is the likely origin of the anomalous conductivity behavior in the more com-

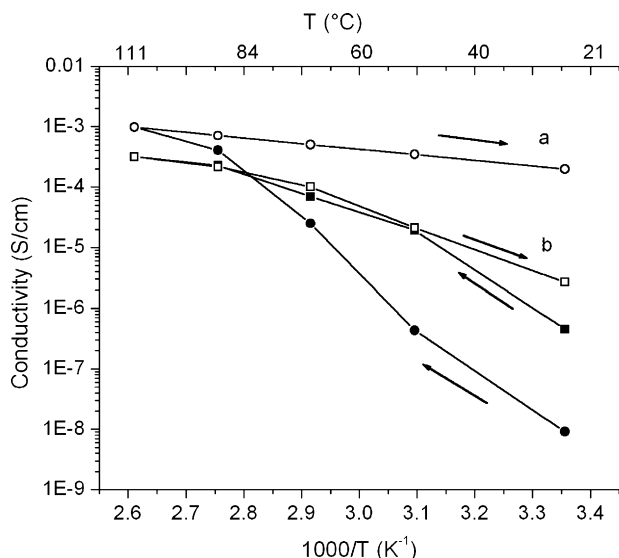


Fig. 3. Conductivity of polymer II. (a) II: LiBF<sub>4</sub> (EO:Li = 5.8:1); (●) heating, (○) cooling; (b) II: LiClO<sub>4</sub> (EO:Li = 5.8:1) (■) heating, (□) cooling.

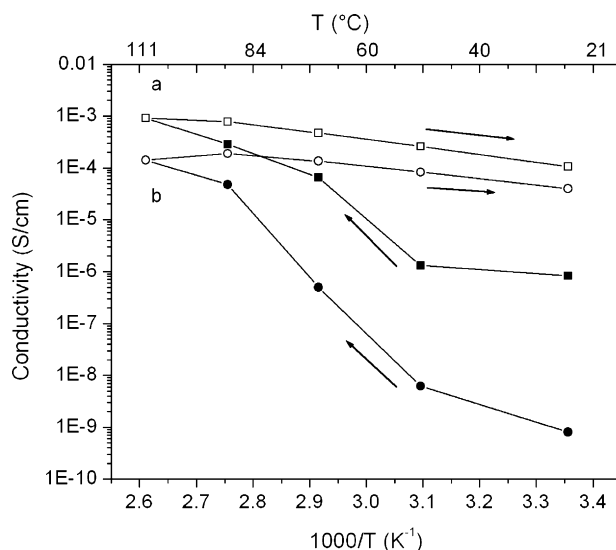


Fig. 4. Conductivity of PTHF. (a) PTHF: LiClO<sub>4</sub> (EO:Li = 5.8:1), (■) heating, (□) cooling; (b) PTHF: LiBF<sub>4</sub> (EO:Li = 5.8:1), (●) heating, (○) cooling.

plex blend systems investigated by Wright and co-workers [7–9] and that the self-organizing properties of polymer I play little role.

Since polytetrahydrofuran (PTHF) is the ion conductive component of polymer II, PTHF homopolymer was synthesized and the temperature dependence of its ionic conductivity investigated. Previously, Alamgir et al. [17] measured the conductivity of PTHF with LiClO<sub>4</sub> salt (EO:Li of 8:1 and 16:1) up to 75 °C. Conductivities and thermal properties of shorter chain length PTHF:LiClO<sub>4</sub> salt systems with various doping levels were reported by Furtado et al. [18] To our knowledge, the conductivity with thermal cycling of PTHF:salt complexes has not been reported to date.

Fig. 4 plots the conductivity of PTHF doped at 5.8:1 EO:Li with LiBF<sub>4</sub> and LiClO<sub>4</sub> as a function of temperature for one heating–cooling cycle. The PTHF:LiBF<sub>4</sub> system exhibits conductivity hysteresis comparable to that observed for the polymer II:LiBF<sub>4</sub> electrolyte, rising from an initial room temperature value  $\sim 10^{-9}$  to  $\sim 10^{-4}$  S/cm after thermal cycling. The data strongly indicate that the PTHF component of polymer II is alone responsible for the weak temperature dependent conductivities reported for blends of I and II [7–9]. Notably, the PTHF:LiClO<sub>4</sub> system also exhibits substantial conductivity hysteresis, with ambient conductivities after thermal cycling above  $10^{-4}$  S/cm.

It was observed that, prior to heat treatment, the polymer II:LiBF<sub>4</sub> electrolyte films were physically heterogeneous, displaying small white precipitates within a translucent matrix. To investigate their thermal behavior, DSC was run on samples taken from both the white and the translucent portions of the film. As shown in Fig. 5, white regions (a) revealed two endotherms, one at 30 °C characteristic of undoped polymer II, and a second, broad endotherm from 90 to 125 °C ( $\Delta H = 56.98$  J/g), which partially recrystallizes (18%), as observed in the DSC cooling trace, to give a weaker endothermic peak at  $\sim 95$  °C on second heating. Samples taken from the translucent film regions (b) exhibited a much weaker high temperature endotherm on initial

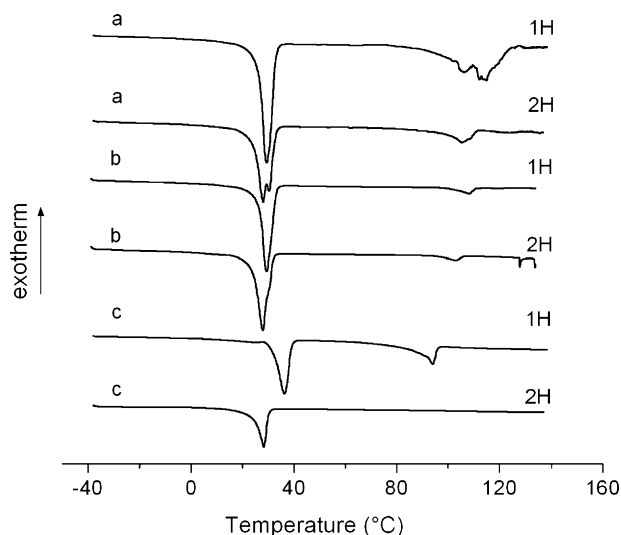


Fig. 5. DSC data for polymer II. (a) White portion of polymer II: LiBF<sub>4</sub>; (b) translucent portion of polymer II: LiBF<sub>4</sub>; (c) polymer II: LiClO<sub>4</sub>; (1H), first heating; (2H) second heating. Samples doped at EO:Li = 5.8:1.

heating ( $\Delta H = 5.26$  J/g), which also only partially recrystallized (13%) on cooling. The conductivity data in Fig. 3 reflect the additive behavior of these different regions of the film.

DSC heating and cooling traces for both PTHF:LiBF<sub>4</sub> and PTHF:LiClO<sub>4</sub> systems are shown in Fig. 6a and b, respectively. The data suggest that regions of high and low salt content coexist in the PTHF:Li salt complexes, despite their optical transparency. The endotherm at 46 °C in Fig. 6b is consistent with the melting point for undoped PTHF reported by Abraham and co-workers [17] as 42 °C, while the high temperature endotherm indicates a second phase of high salt content. The observation of a two-phase polymer:salt system that remains optically clear is consistent with earlier reports by Vachon et al. [19,20] on poly(propylene oxide):lithium salt electrolytes. On second heating, the high temperature endotherm is absent from both PTHF:Li salt complexes (Fig. 6), suggesting these systems exhibit slow recrystallization kinetics.

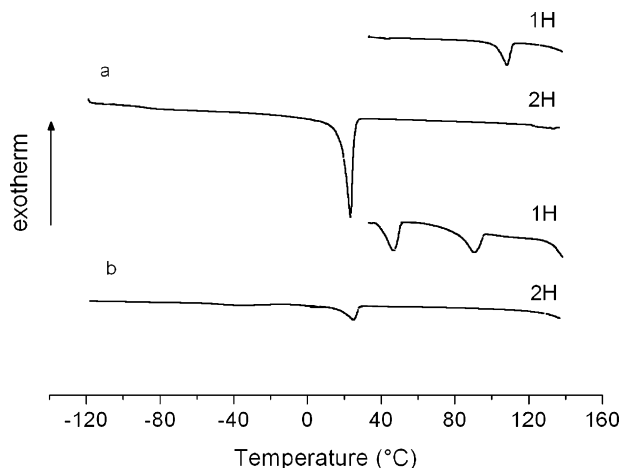


Fig. 6. DSC data for PTHF. (a) PTHF:LiBF<sub>4</sub>; (b) PTHF:LiClO<sub>4</sub>; (1H), first heating; (2H) second heating. Samples doped at EO:Li = 5.8:1.

One might rationally link the absence of recrystallization of the high melting point phase after cooling to the conductivity hysteresis seen for the polymer II:LiBF<sub>4</sub> and PTHF:Li salt systems (Figs. 3 and 4). Indeed, it has been shown that PEO and its composites can exhibit considerable thermal hysteresis in the ionic conductivity as a result of slow crystallization kinetics and thermal treatment history [21–26]. However, DSC measurements on the polymer II:LiClO<sub>4</sub> electrolyte (Fig. 5c) do not support this hypothesis. While these electrolyte films are visibly transparent, DSC traces again show a high melting point endotherm at  $\sim 95$  °C, which does not recrystallize when the sample is cooled. Despite the similarity in its thermal signature to the polymer II:LiBF<sub>4</sub> system and the PTHF:salt complexes, the polymer II:LiClO<sub>4</sub> system demonstrated little hysteresis in conductivity (Fig. 2).

PTHF has been previously reported to decompose to form THF when mixed with lithium salts LiBr and LiI and heated to temperatures above 360 and 280 °C under nitrogen, respectively [27]. Costa et al. [27–29] reported that thermal decomposition of PTHF was enhanced upon complexation with Li<sup>+</sup> salt under N<sub>2</sub> atmosphere. Strong coordination of Li<sup>+</sup> cations with the ether oxygens of PTHF accelerates homolytic C–O bond cleavage to generate macroradicals upon heating. In the absence of O<sub>2</sub>, depropagation proceeds rapidly with the formation of significant quantities of THF monomer once radicals are formed.

To determine whether PTHF decomposition played a role in the observed conductivity behavior of these electrolytes, conductivity samples were retrieved after thermal cycling and subjected to <sup>1</sup>H NMR analysis and GPC. For the polymer II:LiClO<sub>4</sub> electrolyte after two heating–cooling cycles up to 110 °C, the THF content was found to be only 5 wt% from NMR analysis, while the molecular weight decreased moderately from 39 to 32 kg/mol. The retrieved sample was molten in character and did not exhibit a separate liquid phase. By contrast, the decomposition of polymer II when mixed with LiBF<sub>4</sub> was severe. The retrieved sample had a separated liquid fraction after two heating–cooling cycles. <sup>1</sup>H NMR analysis performed on an aliquot containing both liquid and molten phases of the retrieved sample revealed a THF content of 45 wt%, while the polymer molecular weight dropped to 18 kg/mol. The conductivity hysteresis seen in Fig. 3a for polymer II doped with LiBF<sub>4</sub> might thus be explained by the large amount of organic solvent that evolved on heating.

Similarly, PTHF:Li salt complexes experienced considerable decomposition during heating–cooling cycles. NMR analysis revealed 25–35 wt% THF content after two heating–cooling cycles. The molecular weight of LiBF<sub>4</sub>-doped PTHF decreased from 405 to 366 kg/mol after the first heating–cooling cycle and to 180 kg/mol after the second heating–cooling cycle. After removing the solvent in retrieved samples under vacuum at room temperature, the conductivity values dropped to 10<sup>−7</sup> S/cm at room temperature, underlining the pronounced effect of organic solvent on conductivity in these samples.

To differentiate between the effects of slow recrystallization of the high melting point phase and THF evolution on conductivity hysteresis, a PTHF:LiBF<sub>4</sub> complex was heated to 80 °C by placing the conductivity cell into an 80 °C oil bath for 1.5 h. The

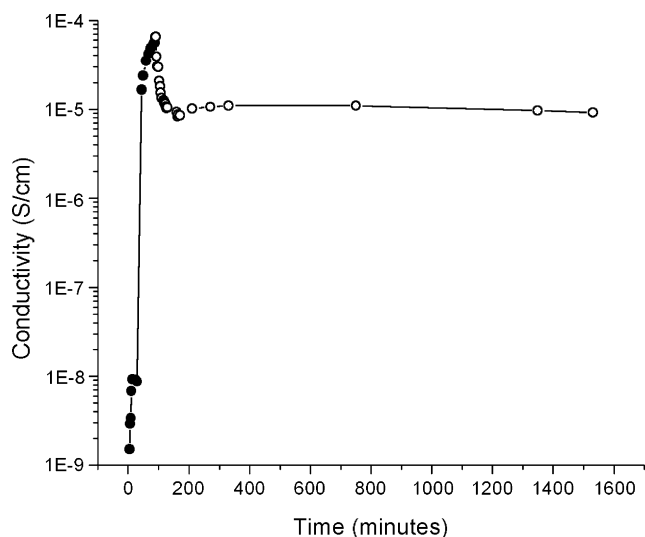


Fig. 7. PTHF:LiBF<sub>4</sub> (EO:Li=5.8:1); (●) immersed in 80 °C oil bath and (○) removed and air cooled to room temperature.

cell was subsequently removed from the bath and cooled to room temperature, during which conductivity data were recorded as a function of time. Although 80 °C resides below the onset of the high temperature endotherm observed for this system seen in the DSC data in Fig. 6a, significant conductivity hysteresis was still observed (Fig. 7). The molecular weight of the retrieved sample was decreased to 275 kg/mol, with 31 wt% THF content by NMR, indicating THF evolution as key to the hysteresis. The drop in conductivity between 100 and 200 min seen in the data of Fig. 7 may be due to phase separation or intermixing of the PTHF and THF, altering the primary conduction pathway. This reduction was not observed in our slow cycling study (Fig. 4), perhaps because the system was provided substantially more time to equilibrate (2–3 h) prior to each conductivity measurement. Nonetheless, the final room temperature conductivity remains nearly four orders of magnitude above the initial value, comparable to the hysteresis observed in Fig. 4 for this system.

Previously reported conductivities for 1 M lithium salt solutions made from various organic solvents fall in the range of  $10^{-2}$  to  $10^{-3}$  S/cm at room temperature, and show weak temperature dependence over decades of degrees [30,31]. The weak temperature dependence of the conductivities observed in our PTHF-containing electrolytes after thermal cycling could be explained by an electrolyte highly swollen with THF or a separated liquid fraction of THF incorporating dissolved lithium salt, and might also account for the high ambient conductivities reported for I:II blends [7–9].

TGA results from PTHF, polymer II and a 50:50 blend of I:II doped with LiBF<sub>4</sub> are displayed in Fig. 8. Samples were equilibrated at 30 °C then ramped to 250 °C in 10 °C/min increments with isothermal holds of 30 min at 70 and 90 °C, and 1 h at 110 °C. Due to differences in heat treatment times and sample environment, the TGA data cannot be compared directly with the THF contents measured after conductivity studies, but do illustrate the susceptibility to decomposition of these polymer–salt systems. Fig. 8 clearly demonstrates weight loss in all three systems during each of the isothermal holds. The

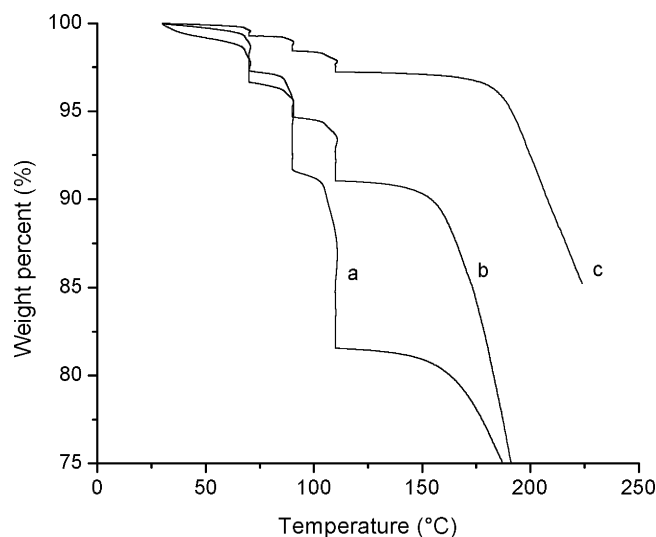


Fig. 8. TGA results for PTHF, polymer II and I:II blend heated in 10 °C/min increments with isothermal holds of 30 min at 70 °C, 30 min at 90 °C and 1 h at 110 °C. (a) PTHF: LiBF<sub>4</sub> (EO:Li=5.8:1); (b) polymer II: LiBF<sub>4</sub> (EO:Li=5.8:1); (c) blend, I: II:LiBF<sub>4</sub> (EO:Li=8:1).

fraction of weight lost tracks with PTHF content—PTHF loses ~18 wt% after the three isothermal holds, while polymer II, having 93.7 wt% PTHF, loses ~9 wt% and the I:II blend, containing 46.8 wt% PTHF, loses ~3 wt%. Decomposition could be expected to exceed these values in conductivity studies in which samples are exposed to elevated temperatures for substantially longer periods.

#### 4. Conclusion

In this work, the mechanism behind the conductivity hysteresis and the resulting weakly temperature dependent conductivities of polymer blend electrolytes reported in a series of recent articles was investigated [7–9]. The poly(tetrahydrofuran) blocks of the polymer II blend component show partial decomposition to THF upon thermal cycling, resulting in a self-plasticizing effect that appears to dominate the shape of the conductivity plot with temperature. Although both polymer II and PTHF when doped with high salt contents form a high melting point phase that shows sluggish recrystallization after thermal cycling, this phenomenon could be ruled out in explaining the observed conductivity hysteresis.

The generation of what is effectively a gel electrolyte in situ through partial decomposition of a polymer suggests a novel processing strategy that could combine the conductivity performance of gels with the processing advantage of polymers. Interestingly, Cataldo [32] recently described a PTHF–THF–iodine gel electrolyte prepared in the converse fashion, i.e., partial polymerization of THF to PTHF via initiation at 80 °C with iodine, which subsequently served as a charge carrier. Room temperature conductivities up to  $\sim 5 \times 10^{-5}$  S/cm were reported for these systems. THF, however, is a highly volatile and flammable solvent, with substantially lower flash and boiling points than plasticizers currently used in gel electrolytes for lithium batteries, such as ethylene carbonate and propylene carbonate, and

is further susceptible to the formation of explosive peroxides. Hence, the self-plasticizing electrolytes described herein are likely to have limited application in lithium batteries.

### Acknowledgements

This work was sponsored by the Office of Naval Research under contract N00014-05-0056 and in part by the MIT MRSEC Program of the National Science Foundation under award DMR-0213282.

### References

- [1] J.M. Tarascon, M. Armand, *Nature* 414 (2001) 359.
- [2] P.V. Wright, *Br. Polym. J.* 7 (1975) 319.
- [3] M. Armand, W. Gorecki, R. Andreani, in: B. Scrosati (Ed.), *Second International Symposium on Polymer Electrolytes*, Elsevier, New York, 1990, p. 91.
- [4] S. Kohjiya, T. Kawabata, K. Maeda, S. Yamashita, in: B. Scrosati (Ed.), *Second International Meeting on Polymer Electrolytes*, Elsevier, New York, 1990, p. 187.
- [5] K. Ito, H. Ohno, *Solid State Ionics* 79 (1995) 300.
- [6] F. Croce, G.B. Appetecchi, L. Persi, B. Scrosati, *Nature* 394 (1998) 456.
- [7] F. Chia, Y. Zheng, J. Liu, N. Reeves, G. Ungar, P.V. Wright, *Electrochim. Acta* 43 (2003) 1939.
- [8] Y. Zheng, J. Liu, Y. Liao, G. Ungar, P.V. Wright, *Dalton Trans.* (2004) 3053.
- [9] J. Liu, Y. Zheng, Y. Liao, X. Zeng, G. Ungar, P.V. Wright, *Faraday Discuss.* 128 (2005) 363.
- [10] Y. Zheng, F. Chia, G. Ungar, T.H. Richardson, P.V. Wright, *Electrochim. Acta* 46 (2001) 1397.
- [11] F.B. Dias, J.P. Voss, S.V. Batty, P.V. Wright, G. Ungar, *Macromol. Rapid Commun.* 15 (1994) 961.
- [12] F.B. Dias, S.V. Batty, G. Ungar, J.P. Voss, P.V. Wright, *J. Chem. Soc. Faraday Trans.* 92 (14) (1996) 2599.
- [13] F.B. Dias, S.V. Batty, J.P. Voss, G. Ungar, P.V. Wright, *Solid State Ionics* 85 (1996) 43.
- [14] Y. Zheng, F. Chia, G. Ungar, P.V. Wright, *Chem. Commun.* (2000) 1459.
- [15] Y. Zheng, F. Chia, G. Ungar, P.V. Wright, *J. Power Sources* 97–98 (2000) 641.
- [16] F.S. Chia, Y. Zheng, G. Liu, G. Ungar, P.V. Wright, *Solid State Ionics* 147 (2002) 275.
- [17] M. Alamgir, R.T. Moulton, K.M. Abraham, *Electrochim. Acta* 36 (1991) 773.
- [18] C.A. Furtado, G. Silva, M.A. Pimenta, J.C. Machado, *Electrochim. Acta* 43 (1998) 1477.
- [19] C. Vachon, M. Vasco, M. Perrier, J. Prud'homme, *Macromolecules* 26 (1993) 4023.
- [20] C. Vachon, C. Labrèche, A. Vallée, S. Besner, M. Dumont, J. Prud'homme, *Macromolecules* 28 (1995) 5585.
- [21] B. Choi, Y. Kim, *Electrochim. Acta* 49 (2004) 2307.
- [22] J.E. Weston, B.C.H. Steele, *Solid State Ionics* 2 (1981) 347.
- [23] F. Croce, G.B. Appetecchi, C. Persi, B. Scrosati, *Nature* 394 (1998) 456.
- [24] B. Kumar, L.G. Scanlon, *Solid State Ionics* 124 (1999) 239.
- [25] B. Kumar, S. Koka, S.J. Rodrigues, M. Nookala, *Solid State Ionics* 156 (2003) 163.
- [26] B. Kumar, L.G. Scanlon, R. March, R. Mason, R. Higgins, R. Baldwin, *Electrochim. Acta* 46 (2001) 1515.
- [27] L. Costa, M.P. Luda, G.G. Cameron, M.Y. Qureshi, *Polym. Deg. Stab.* 67 (2000) 527.
- [28] L. Costa, A.M. Gad, G. Camino, G.G. Cameron, M.Y. Qureshi, *Macromolecules* 25 (1992) 5512.
- [29] L. Costa, G. Camino, M.P. Luda, G.G. Cameron, M.Y. Qureshi, *Polym. Deg. Stab.* 48 (1995) 325.
- [30] M. Alamgir, K.M. Abraham, in: G. Pisotia (Ed.), *Lithium batteries: New materials, Developments and Perspectives*, Elsevier, Amsterdam, New York, 1994 (chapter 3).
- [31] G.M. Ehrlich, in: D. Linden, T.B. Reddy (Eds.), *Handbook of Batteries*, third ed., McGraw-Hill, New York, 2002 (chapter 35).
- [32] F. Cataldo, *Solid State Ionics* 139 (2001) 281.